Marine Micropaleontology 109 (2014) 30–45

Contents lists available at ScienceDirect

Marine Micropaleontology

journal homepage: www.elsevier.com/locate/marmicro

Research paper

A quantitative analysis of calcareous nannofossil bioevents of the Late Cretaceous (Late Cenomanian–Coniacian) Western Interior Seaway and their reliability in established zonation schemes

M.J. Corbett [a,*], D.K. Watkins [a], J.J. Pospichal [b]

[a] Department of Earth and Atmospheric Sciences, University of Nebraska–Lincoln, Lincoln, NE 68588-0340, USA
[b] BugWare Oilfield Paleontology, 1615 Village Square Rd., Suite #8, Tallahassee, FL 32309, USA

ARTICLE INFO

Article history:
Received 26 April 2013
Received in revised form 3 April 2014
Accepted 13 April 2014
Available online 26 April 2014

Keywords:
Calcareous nannofossils
Biostratigraphy
Ranking and Scaling
Late Cretaceous
Western Interior Basin

ABSTRACT

Calcareous nannofossil assemblages from 8 localities in the Upper Cenomanian–Coniacian strata of central (Colorado and Kansas) and southern (Texas) Western Interior Seaway, USA were analyzed to produce a new high resolution biostratigraphic framework for the Greenhorn Formation, Eagle Ford Formation, and basal Austin Chalk. Eighteen datasets from coeval successions around the world, including the Global Stratotype Section and Point (GSSP) at Pueblo, CO and proposed reference sections for the base of the Turonian and candidate GSSPs for the base of the Coniacian in Germany, Poland, and New Mexico, were incorporated from literature sources. Additional discussion is devoted to the basal Turonian and Coniacian boundaries as they reflect paleoceanographic phenomena (e.g. OAE2, widespread Late Turonian regression) where high-resolution biostratigraphy has academic, as well as industrial, application.

Ranking and Scaling of 48 selected bioevents produces a quantitatively derived optimum sequence of first and last occurrences. Scaling of events along a relative time-scale reveals an 8–9% evolutionary turnover during OAE2. Comparison with the qualitatively developed nannofossil zonations known as the CC zonation of Perch-Nielsen and UC zonation of Burnett reveals inconsistencies, largely due to the recognition of new/amended species concepts. Discrepancies near the Turonian/Coniacian boundary reflect changes to its placement in recent revisions to the geologic timescale. A recently documented sequence of bioevents provides an accurate proxy for the boundary in the absence of the inoceramid index fossil *Cremnoceramus deformis erectus* (Meek). Fifteen bioevents from the optimum sequence are given greater priority based on their interpreted reliability between the sections examined and the CC and UC zonations.

1. Introduction

Numerous authors (e.g., Watkins, 1985, 1986; Bralower, 1988; Bralower and Bergen, 1998; Burns and Bralower, 1998; Sikora et al., 2004; Eleson and Bralower, 2005; Desmares et al., 2007) have examined the mid–late Cretaceous calcareous nannofossil biostratigraphy and paleoecology of the central region of the Western Interior; however, very few investigations (Smith, 1981; Jiang, 1989) have documented their record at the seaway's southern aperture. We present a high-resolution Upper Cenomanian through Coniacian biostratigraphy from 8 sites (Fig. 1) across the southern and central Western Interior Basin (WIB). These observations enable us to construct the first detailed stratigraphic framework based on calcareous nannofossil bioevents for the Eagle Ford Formation and basal Austin Chalk and compare it to new and previously published datasets from the Greenhorn and Niobrara formations in the central WIB.

The Western Interior Basin is a north–south oriented foreland basin which formed through flexural subsidence during the Sevier Orogeny (Kauffman and Caldwell, 1994). During the Mid-to-Late Cretaceous, the WIB was inundated by a shallow seaway, the Western Interior Seaway. The shallow, epeiric setting resulted in a stratigraphic record strongly influenced by regional tectonism and global fluctuations in sea-level. Biostratigraphic analysis of calcareous nannofossils can provide a high resolution framework to correlate the distinct facies and stratigraphic sequences deposited in the WIB to equivalent successions and zonal schemes developed in deep marine settings (e.g. Bralower and Bergen, 1998; Corbett et al., 2011; Donovan et al., 2012).

Calcareous nannoplankton evolved and spread rapidly across the world's oceans during the Cretaceous, making their evolutionary first occurrences (or lowest occurrence, LO) and extinction events (or highest occurrence, HO) excellent markers for regional and global correlations. Species whose LO or HO occurs abruptly and synchronously

* Corresponding author. Tel.: +1 781 771 0596.
E-mail address: mcorbett@huskers.unl.edu (M.J. Corbett).

http://dx.doi.org/10.1016/j.marmicro.2014.04.002
0377-8398/

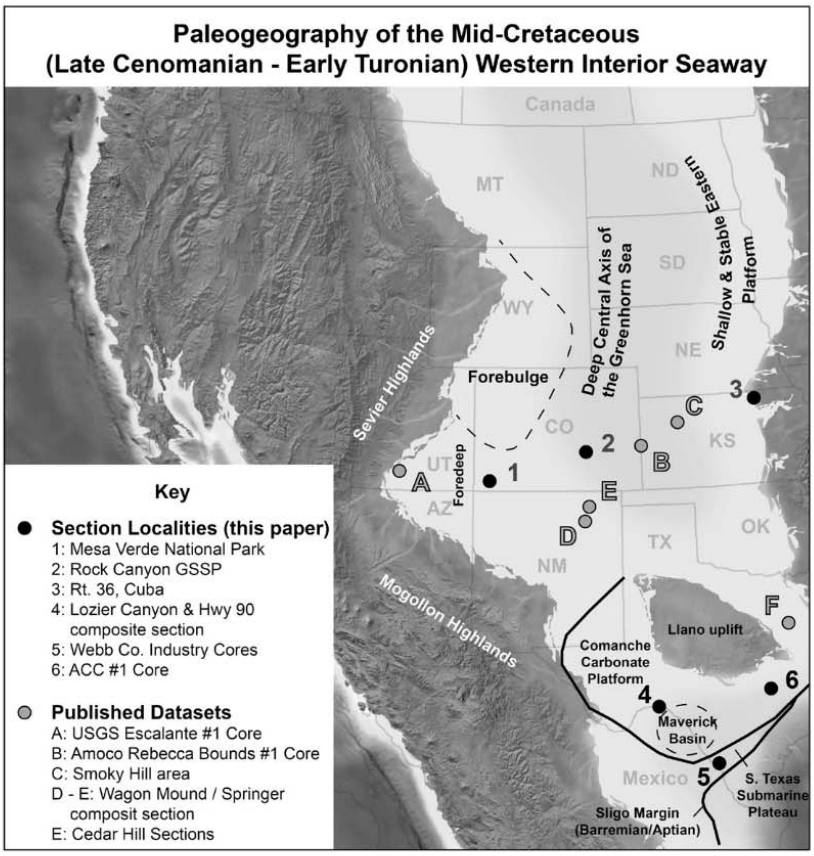

Fig. 1. Paleogeographic map of western North America approximately during peak transgression of the Western Interior Seaway in the Late Cenomanian–Early Turonian. Paleoceanographic features from the central and southern regions of the seaway are reconstructed from Leckie et al. (1998) and Donovan et al. (2012), respectively. Localities of sections examined in this paper are labeled with dark filled circles, while datasets from the existing literature are marked with gray labels.
Modified from Blakey (2012).

across many localities may be used as biostratigraphic datums. Zonation schemes have been developed (e.g. Fig. 2; CC zonation: Perch-Nielsen, 1985; UC zonation: Burnett, 1998), based on interpretation and comparison of biostratigraphic events in regional or global datasets and are often tied to the geologic timescale through absolute dating methods (e.g., radiogenic isotopes) or other proxies (e.g., isotope records, magnetostratigraphy).

Qualitative and quantitative statistical analyses of a series of nannofossil events from WIB localities and 18 additional datasets from around the world facilitate the development of an optimal sequence of biostratigraphic datums (Table 1 in the online Supplementary Data, Appendix B). This statistically derived sequence of events is contrasted with the widely used CC zonal scheme developed by Perch-Nielsen (1985) and a later modified version, the UC scheme of Burnett (1998), which contains many additional subzones and secondary markers. The CC and UC schemes are summarized in Fig. 2, with modifications based on different species concepts and updates to zonations discussed herein (1.2.; 4.3., 4.4.). Particular attention is devoted to two stratigraphic intervals: the Upper Cenomanian to Lower Turonian Oceanic Anoxic Event 2 and the Coniacian stage boundary.

2. Localities and regional setting

Three exposures of the Cenomanian–Turonian Greenhorn Formation from the central WIB and six sites from outcrops and subsurface cores of the Cenomanian–Coniacian Eagle Ford Formation and Austin Chalk from the southern aperture of the Western Interior Seaway are analyzed herein. Their locations, as well as the location of previously published nannofossil datasets from the WIB, are plotted in Fig. 1. The Cenomanian–Turonian boundary GSSP site is located in the central WIB along a railroad embankment in Rock Canyon, near Pueblo, Colorado (Figs. 1, 3B). Exposures of equivalent age are found at Mesa Verde National Park in southwest Colorado (Figs. 1, 3A) and north-central Kansas (Figs. 1, 3C). Roadcuts and streams expose large outcroppings of mid-to-upper Cretaceous rocks in a wide band across Texas, and water and industry drillcores capture this succession in the subsurface. Texas sites included here consist of: a composite section between outcrops in Lozier Canyon, Terrell Co. (Fig. 4A) and Hwy 90 near Langtry, Val Verde Co. (Fig. 4B); subsurface samples from the ACC #1 core, Travis Co. (Fig. 4C); and subsurface samples from the Fasken "A" #1-H, Chamberlain State, and Saunders 108 1-H cores

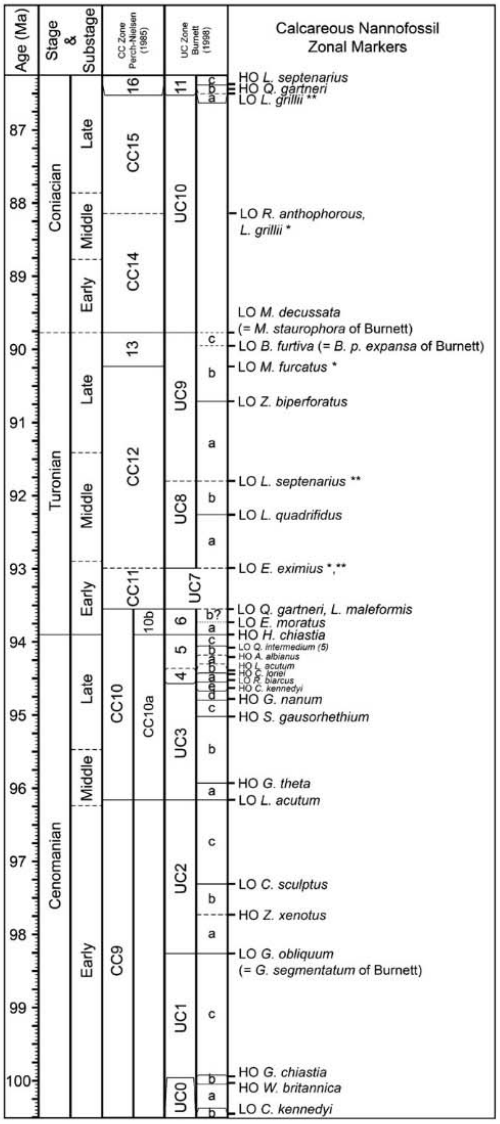

Fig. 2. A summary of the widely used CC and UC nannofossil zonations developed by Perch-Nielsen (1985) and Burnett (1998), respectively. Placement of zones and bioevents in geologic time is based on updated timescale of Ogg and Hinnov (2012). Use or placement of events specific to either scheme is indicated by asterisks (*CC, **UC). Species concepts used by either author are also indicated.
Created using TSCreator, Ogg and Lugowski (2013).

(Fig. 5) from Webb Co. For a more detailed description of the sections studied please look into the supplementary content (Appendix C).

Calcareous nannofossil and chemostratigraphic events can be correlated between these localities to construct two relatively proximal to distal cross-sections for the central and southern WIB. Rock Canyon was located in the deepest part of the foreland basin at an estimated 175–300 m depth during peak transgression while Mesa Verde was in a more proximal setting with a shallow, distal epieric setting to the east in Kansas (Sageman and Arthur, 1994). The three industry cores in Webb Co., Texas reveal an expanded and relatively complete Cenomanian through Coniacian succession deposited on a submarine shelf downdip of the Cretaceous Comanche carbonate platform that covered much of the southern WIB (Donovan et al., 2012). Lozier Canyon and the ACC #1 core are more condensed sections deposited atop the carbonate platform where unconformities are more prevalent (Donovan et al., 2012).

Eighteen additional datasets from localities around the globe were included in our quantitative statistical analysis of calcareous nannofossil events from the Upper Cenomanian through Coniacian (Table 1). These supplementary sites are found in the central Western Interior, northern and equatorial Atlantic, equatorial Pacific, United Kingdom, Europe, and Morocco. The sources of these previously studied sites are summarized in Table 1.

3. Methods

Calcareous nannofossil biostratigraphic events were recorded using a Zeiss Photoscope III at a total magnification of 1250× using cross-polarized light, plane light, phase contrast, and through a one-quarter □ mica plate. Outcrop and core samples were prepared using the double slurry and settling methods for making microscope slides detailed by Geisen et al. (1999) and Watkins and Bergen (2003). The cascading counting technique developed by Styzen (1997) was used to collect assemblage data for most sample sets and additional traverses were made to locate especially rare species. Data are archived at the World Data Center-A for Paleoclimatology http://www.ncdc.noaa.gov/paleo/data.html (Corbett et al., submitted for publication).

Ranking and Scaling (RASC) is a probabilistic method largely developed by F.P. Agterberg and F.M. Gradstein (Gradstein et al., 1985; Agterberg and Gradstein, 1999). RASC uses a randomized algorithm to rank a series of events (first appearance datums, or FADs, and last appearance datums, or LADs, etc.) and separately scales them within a sequence using the frequency of cross-over and co-occurrence between event pairs. It follows a "majority rule" calculation and instead of preferentially maximizing a biostratigraphic datum, as in deterministic methods (e.g. CONOP total range method), RASC uses an average of all observed occurrences across the dataset (Kemple et al., 1995; Agterberg and Gradstein, 1999). Occasional errors can occur by allowing range contractions, but frequently results in producing a precise optimum sequence (Hammer and Harper, 2006). A detailed description of the statistical method can be found in Agterberg and Gradstein (1999) and Hammer and Harper (2006).

Ranking and Scaling was performed using the statistical software program PAST on 26 datasets including the new information presented here and biostratigraphic information from the published literature (Tables 1–3 in the online Supplementary Data). A threshold for observations of an event was set to 3 so that a biostratigraphic datum had to occur in at least ~10% of all of the sites included to be incorporated into the RASC analysis. The average number of observations for the events included in the analysis is 8.8, or approximately 34% of the 26 sites. Additional sources containing calcareous nannofossil biostratigraphic data with information recording the vertical thickness separation between samples in outcrop or core were catalogued into a spreadsheet for RASC (Appendix B). A set of 48 events was selected from the Cenomanian through Coniacian that is largely composed of calcareous nannofossil datums either already used in regional or global zonal schemes or events chosen to test their possible biostratigraphic usefulness. Several supplementary datums were added to enable comparisons to the geologic timescale through OAE2.

As a result of the increased burial of organic carbon, OAE2 is also marked by a distinct 2–5‰ □^{13}C excursion in marine carbonates (Pratt, 1985; Arthur et al., 1988; Kennedy et al., 2005). This excursion

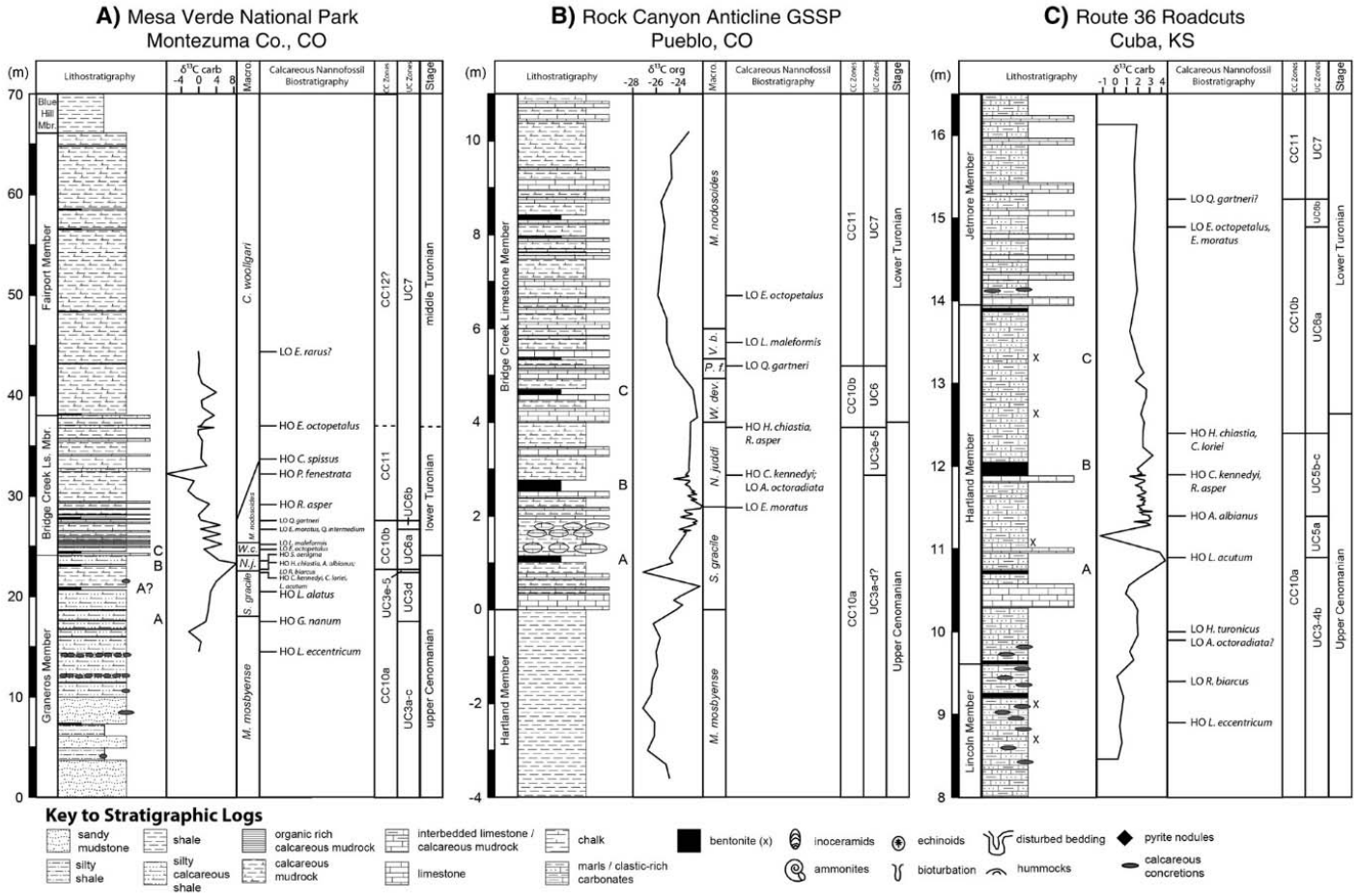

Fig. 3. Stratigraphic logs, calcareous nannofossil biostratigraphy, and carbon isotope values of sections studied from the central Western Interior Basin. Nannofossil bioevents have been used to interpret CC (Perch-Nielsen, 1985) and UC (Burnett, 1998) zonations. The stratigraphic log and macrofossil zonation for Mesa Verde are modified from Leckie et al. (1997) and for Rock Canyon from Kennedy et al. (2005). The stratigraphic log for Cuba is modified from Hattin (1975a, 1975b). Carbon isotope values for Cuba and Rock Canyon are from Bowman and Bralower (2005). Letters A, B, and C indicate interpreted placement of bentonite marker beds of Elder (1985).

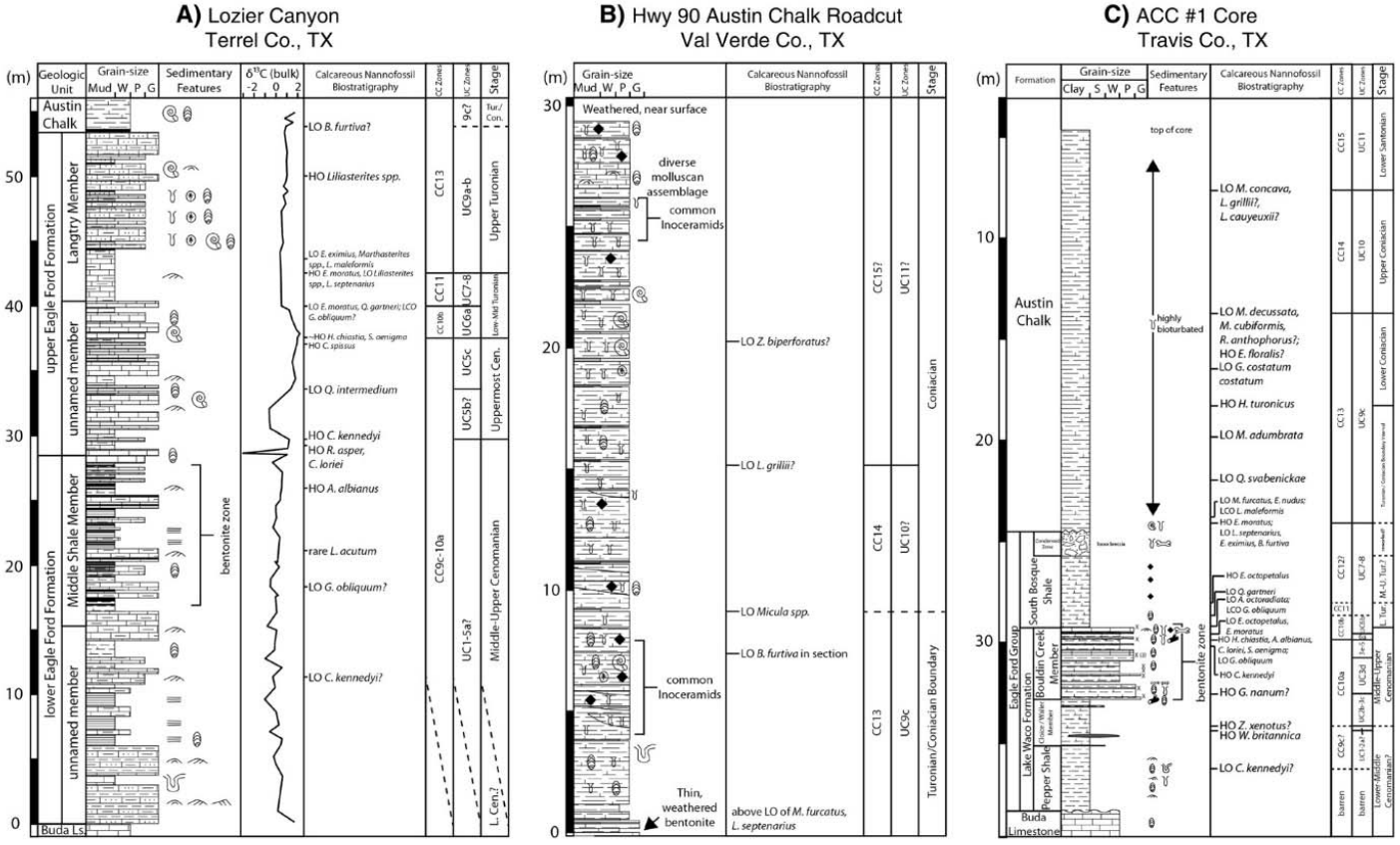

Fig. 4. Stratigraphic logs, calcareous nannofossil biostratigraphy, and carbon isotope values of sections studied from the central Western Interior Basin. Nannofossil bioevents have been used to interpret CC (Perch-Nielsen, 1985) and UC (Burnett, 1998) zonations (Fig. 2). The stratigraphic log and carbon isotope values from Lozier Canyon are modified from Donovan et al. (2012) and Lowery et al. (in review).

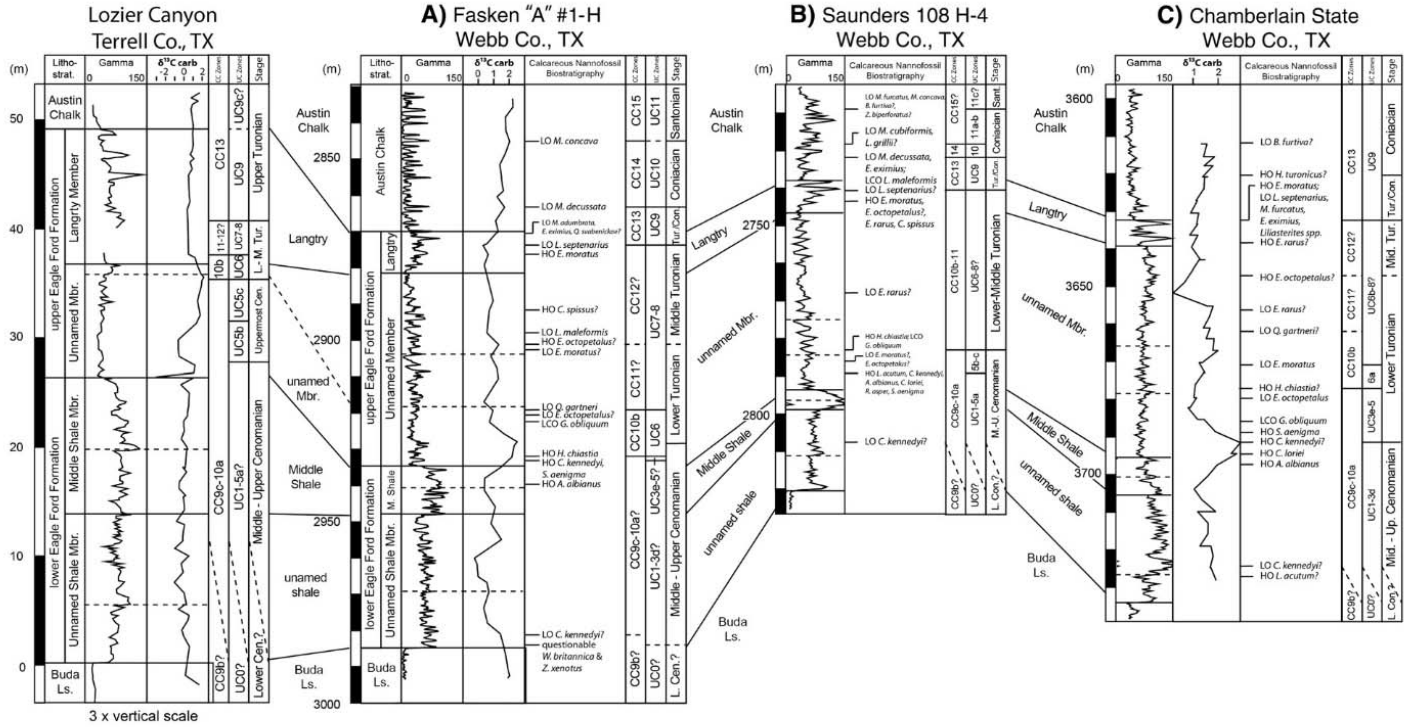

Fig. 5. Gamma ray profiles, calcareous nannofossil biostratigraphy, and carbon isotope values of sections studied from the southern Western Interior Basin. Nannofossil bioevents have been used to interpret CC (Perch-Nielsen, 1985) and UC (Burnett, 1998) zonations (Fig. 2). Solid lines between sections indicate correlations of member and formation boundaries based on interpretations of the gamma ray logs and calcareous nannofossil biostratigraphy. The gamma ray profile from Lozier Canyon and the Fasken "A" #1-H core are modified from Donovan et al. (2012) as well as carbon isotope values for Lozier Canyon.

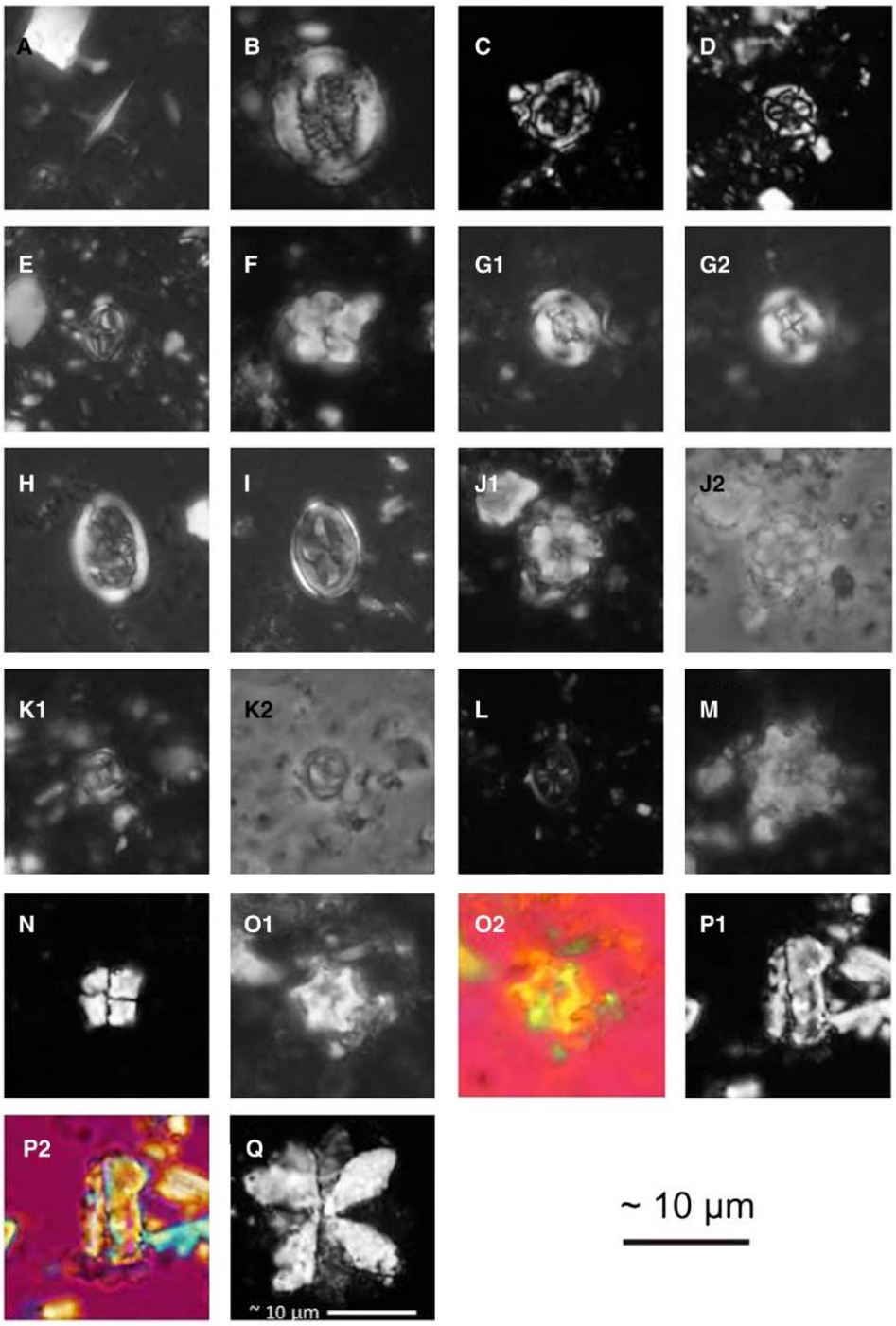
A
B
C
D
E
F
G1
G2
H
I
J1
J2
K1
K2
L
M
N
O1
O2
P1
P2
Q
~ 10 µm
~ 10 µm

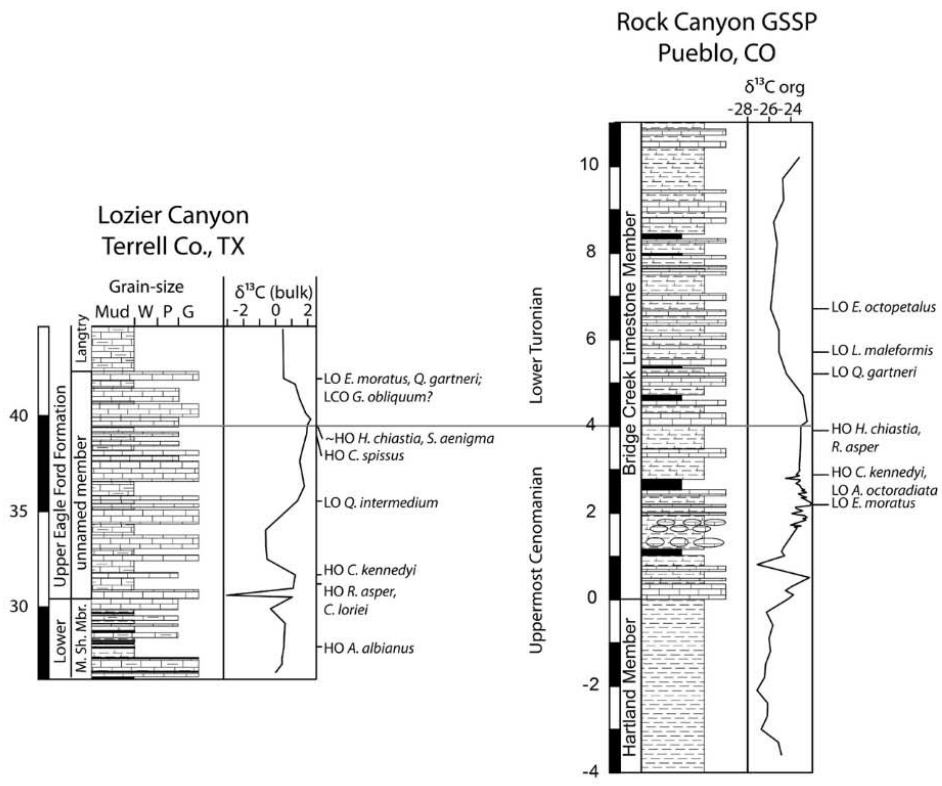

Fig. 6. Comparison of biostratigraphic events and carbon isotope stratigraphy between Lozier Canyon, TX and Rock Canyon Anticline, Pueblo, CO showing the placement of the base Turonian Stage boundary. Carbon isotope stratigraphy and stratigraphic log from Lozier Canyon modified from Donovan et al. (2012) and Rock Canyon from Bowman and Bralower (2005) and Kennedy et al. (2005).

has been tied to the geologic timescale at the Cenomanian–Turonian GSSP at Pueblo, CO and a European reference section (Kennedy et al., 2005; Jarvis et al., 2006). Carbon isotope curves previously generated by Bowman and Bralower (2005) are used for Pueblo, CO Cuba, KS sections. These samples are coeval for the Rock Canyon, Pueblo outcrop but are more detailed in the isotope sampling for Cuba. Carbon isotope curves were generated in parallel with the current work by Donovan et al. (2012) and Lowery et al. (in review) for Lozier Canyon, and the Fasken Core. These additional events allow for a detailed calibration between biostratigraphic and chemostratigraphic events from the upper Cenomanian through the lower Turonian (e.g., Hardas and Mutterlose, 2006; Linnert et al., 2010). The LO of inoceramid *Cremnoceramus deformis erectus* at 4 localities is also included as a proxy for the base of the Coniacian stage.

Nannofossil events and carbon isotope stratigraphy are correlated between outcrops along Lozier Canyon in Terrell Co. and subsurface cores from Webb and Travis Co. Texas to create a cross-section between the South Texas Submarine Plateau, Comanche Platform, and the Llano highlands (Figs. 4–5). A second cross-section was produced between sites from southwestern Colorado to north-central Kansas (Fig. 3). Events recognized across the WIB are contrasted with established zonation schemes and previously published biostratigraphic work from other successions around the world.

4. Results

4.1. Mesa Verde National Park, CO

Forty-one samples originally collected by Leckie et al. (1998) were used for nannofossil biostratigraphic analysis through the Graneros and Bridge Creek members of the Mancos Shale at Mesa Verde. Calcareous nannofossils are relatively abundant and poor to moderately preserved through this section. A detailed description of the interpreted CC zonation and key marker taxa is found in Corbett and Watkins (in

Plate 1. Light photomicrographs of select calcareous nannofossils from the Late Cenomanian–Upper Turonian RASC optimum sequence at 1250× magnification. XPL = cross-polarized light. PH = phase contrast. GYP = gypsum plate. *L. acutum*, U. Cenomanian, 11.4 m, Mesa Verde, CO; XPL. *C. loriei*, L.-M. Cenomanian, 35.66 m, ACC #1, TX: XPL. *A. albianus*, M.-U. Cenomanian, 21.1 m, Lozier Canyon, TX; XPL. *C. kennedyi*, M.-U. Cenomanian, 28.5 m, Lozier Canyon, TX; XPL. *S. aenigma*, U. Cenomanian, 16.5 m, Mesa Verde, CO; XPL. *Q. intermedium*, L. Turonian, 27.6 m, Mesa Verde, CO; XPL. *H. chiastia*, U. Cenomanian, 12 m, Mesa Verde, CO; G1–2: XPL, high through low focus. *R. asper*, U. Cenomanian, 5.8 m, Mesa Verde, CO; XPL. *G. obliquum*, U. Cenomanian, 12 m, Mesa Verde, CO; XPL. *E. octopetalus*, L. Turonian, 27.1 m, Mesa Verde, CO; J1: XPL, J2: PH. *R. biarcus*, L. Turonian, 28.1 m, Mesa Verde, CO; K1: XPL, K2: PH. *A. octoradiata*, Turonian, 24.69 m, ACC #1, TX; XPL. *E. moratus*, L.-M. Turonian, 42.5 m, Lozier Canyon, TX; XPL. *Q. gartneri*, U. Turonian, 48.46 m, Lozier Canyon, TX; XPL. *E. rarus*, M. Turonian, 44.4 m, Mesa Verde, CO; O1: XPL, O2: GYP. *L. maleformis*, Uppermost Turonian, 54.4 m, Lozier Canyon, TX; P1: XPL, P2: GYP. *Q. giganteum*, U. Turonian, 44.8 m, Lozier Canyon, TX; XPL.

pressa). The HO of *Helenia chiastia*, *Corollithion kennedyi*, *Cretarhabdus loriei* (Plate 1, Fig. B), and *Axopodorhabdus albianus* (Plate 1, Fig. C) occurs just below the base of the Bridge Creek Limestone Member, at the contact between the Upper Cenomanian and Lower Turonian *Sciponoceras gracile* and *Neocardioceras juddi* ammonite zones (Leckie et al., 1997). *Quadrum gartneri* is observed ~3 m higher in the section. The HO of *Eprolithus octopetalus* is observed approximately 3 m above the interpreted base of the Middle Turonian *Collignoniceras wollgari* zone near the top of the Bridge Creek Member.

4.2. Rock Canyon, Pueblo, CO

Fifty-eight samples from the Bridge Creek Member at Rock Canyon were analyzed for biostratigraphic events (Fig. 3B). Preservation is moderate to poor and nannofossils are common. Additional data on the Bridge Creek Member and underlying Hartland Member from Watkins (1985) were incorporated into this analysis. The LO of *Q. gartneri* (Plate 1, Fig. N) and HO of *H. chiastia* (Plate 1, Fig. G) are found within 1–2 m of the base of the Turonian boundary in bed 86. Six additional nannofossil datums are observed within the interval of OAE2 including the LOs of *Eprolithus moratus* (Plate 1, Fig. M), *E. octopetalus* (Plate 1, Fig. J), *Ahmuellerella octoradiata* (Plate 1, Fig. L), and *Lucianorhabdus maleformis* (Plate 1, Fig. P), and HOs of *C. kennedyi* (Plate 1, Fig. D) and *Rhagodiscus asper* (Plate 1, Fig. H).

4.3. Route 36, Cuba, KS

Sixteen samples were analyzed from ~6.8 m of section through the Lincoln, Hartland, and Jetmore members of the Greenhorn Formation from northeast of Cuba, KS. Nannofossils are generally poorly preserved, but common. *H. chiastia* last occurs between 12.4 and 12.9 m in the middle of the Hartland Member and near the top of the plateau in the carbon isotope excursion. *Q. gartneri* is very rare at Cuba. The lowest occurrence of *Q. gartneri* is at 15.23 m in the Jetmore Member, some 2–3 m above the base of the Turonian. All 13 nannofossil bioevents observed in samples from Cuba, KS are shown in Fig. 3C.

4.4. Lozier Canyon/Hwy 90 Composite section, Terrell and Val Verde Co., TX

A total of 57 samples were collected from a ~57 m exposure of the Eagle Ford Formation and basal Austin Chalk in Lozier Canyon. Nannofossils are very poorly preserved in the lower Eagle Ford Formation and samples are barren in the lower ~3 m of the upper Eagle Ford Formation. Preservation increases in the Langtry Member and calcareous nannofossil assemblages are more diverse, but return to very poor preservation in the overlying Austin Chalk. A detailed analysis of the microfossil biostratigraphy and foraminiferan paleoecology from Lozier Canyon is found in Lowery et al. (in review).

Calcareous nannofossil events are consistent with observations near the Cenomanian–Turonian boundary at Rock Canyon. The base of the Turonian Stage can be correlated between Lozier Canyon and Rock Canyon by interpreting the characteristic pattern of carbon isotope values, which are plotted with nannofossil events in Fig. 6. The LO of *Q. gartneri* and HO of *H. chiastia* straddle the top of a carbon isotope excursion ~10 ft below the Langtry Member. The HO of *C. kennedyi*, *R. asper*, *C. loriei*, and *A. albianus* coincides with the base of the OAE2 excursion at the contact between the lower and upper parts of the Eagle Ford Formation.

A disconformity bearing rip-up clasts and shell debris at the base of the Langtry Member is interpreted as a sequence boundary by Donovan et al., 2012. The LO of *Marthasterites furcatus* (Plate 2, Fig. G), *Lithastrinus septenarius* (Plate 2, Fig. D) and the genus *Liliasterites* (Plate 2, Fig. A) is observed less than 3 m above this surface. The LO of *Broinsonia furtiva* (Plate 2, Fig. E; Hattner and Wise, 1980) is observed just above the base of the Austin Chalk.

An additional 33 samples were collected from roadcuts through nearly 30 m of the Austin Chalk about 15 mi to the east in Val Verde Co. Several calcareous nannofossil events were observed despite very poor preservation. The LO of *Micula* spp. occurs ~9 m above the base of the Austin Chalk and *B. furtiva* is found ~7.5 m above the base, although it appears lower at the base of the Austin in Lozier Canyon. The LO of *Lithastrinus grillii* (Plate 2, Fig. K) is found at ~15 m and the LO of *Zeugrhabdotus biperforatus* (Plate 2, Fig. F) is found at ~20.2 m.

4.5. ACC #1 core, Travis Co., TX

Calcareous nannofossils from the top of the Buda Limestone, the Eagle Ford Formation and Austin Chalk in the ACC #1 core were analyzed in 73 samples (Fig. 4C). Samples were barren of nannofossils through the Buda and most of the Pepper Shale Member. Nannofossil becomes abundant in the upper part of the Pepper Shale Member and is well-to-moderately preserved in the calcareous mudrocks of the Cloice and South Bosque Shale Members. Preservation is poor in the more limestone-dominated Bouldin Creek Member and the Austin Chalk.

There are few nannofossil events recognized below the Bouldin Creek Member, while many occur in a very condensed interval less than a meter from the top of the Bouldin Creek Member (Fig. 4C). The HO of *Zeugrhabdotus xenotus* and *Watznaueria britannica* occurs in the Cloice Member. The HO of *C. kennedyi*, *A. albianus*, and *H. chiastia* and the LO of *E. moratus* and *E. octopetalus* are found less than half a meter from an erosional contact. Carbon isotope data were not available for the core, but the analyses of nearby cores by Fairbanks and Ruppel (2012) show no distinct excursion associated with OAE2.

Several nannofossil events coincide with another erosional contact at the base of the Austin Chalk. The LO of *L. septenarius*, *M. furcatus*, and *B. furtiva* is observed at or just above this surface. The LO of *Micula decussata* (= *M. staurophora*) (Plate 2, Fig. J) occurs ~10 m above the base of the Austin Chalk. The LO of *Micula adumbrata* (Plate 2, Fig. I) and HO of *Helicolithus turonicus* (Plate 2, Fig. H) occur between the LO of *B. furtiva* and *M. decussata* in the lower 4–6 m of the Austin Chalk.

4.6. Fasken "A" #1-H, Chamberlain State, Saunders 108 H-4: Webb Co., TX

A total of 138 samples were collected from three petroleum industry cores in Webb Co., TX: 57 from the Fasken "A" #1-H, 44 from the Chamberlain State, and 37 from the Saunders 108 H-4 (Fig. 5). Nannofossil preservation is generally poor to very poor throughout these cores. Approximately 23–38 m from the top of the Buda Limestone is a 7–15 m thick interval of high gamma ray response. The HO of *C. kennedyi*, *A. albianus*, and *C. loriei* occurs just above this interval in a lower gamma facies, which appears consistent with the wireline log contact between the Middle Shale and unnamed member in the upper Eagle Ford at Lozier Canyon and the Bouldin Creek Member in the ACC #1 core.

Carbon isotope data from the Fasken "A" #1-H and Chamberlain State, while relatively low resolution, reveal a 2–3‰ excursion above the high gamma facies, which is also consistent with the interpreted stratigraphic interval containing OAE2 at Lozier (Fig. 5). The end of this excursion, before values begin to recover, is nearly 30–60 m above the base of the Eagle Ford. The HO of *H. chiastia*, while found slightly lower in the Fasken core, occurs at about this level in the Chamberlain State and Saunders 108 H-4 cores near the LO of *E. octopetalus* and *E. moratus*. *Q. gartneri* is very rare in the Chamberlain and Saunders, but can be found just above this interval in the Fasken. In the Chamberlain and Saunders Webb Co. cores *Eprolithis rarus* (Plate 1, Fig. O) occurs above the top of the Middle Shale high gamma facies. In the early part of its range *Gartnerago obliquum* is rare and not observed consistently between samples. Across all 5 sites in Texas *G. obliquum* increases in abundance near the Cenomanian–Turonian boundary. This event appears to be a reliable datum in lieu of some of the rarer Upper Cenomanian–Lower Turonian taxa in Texas.

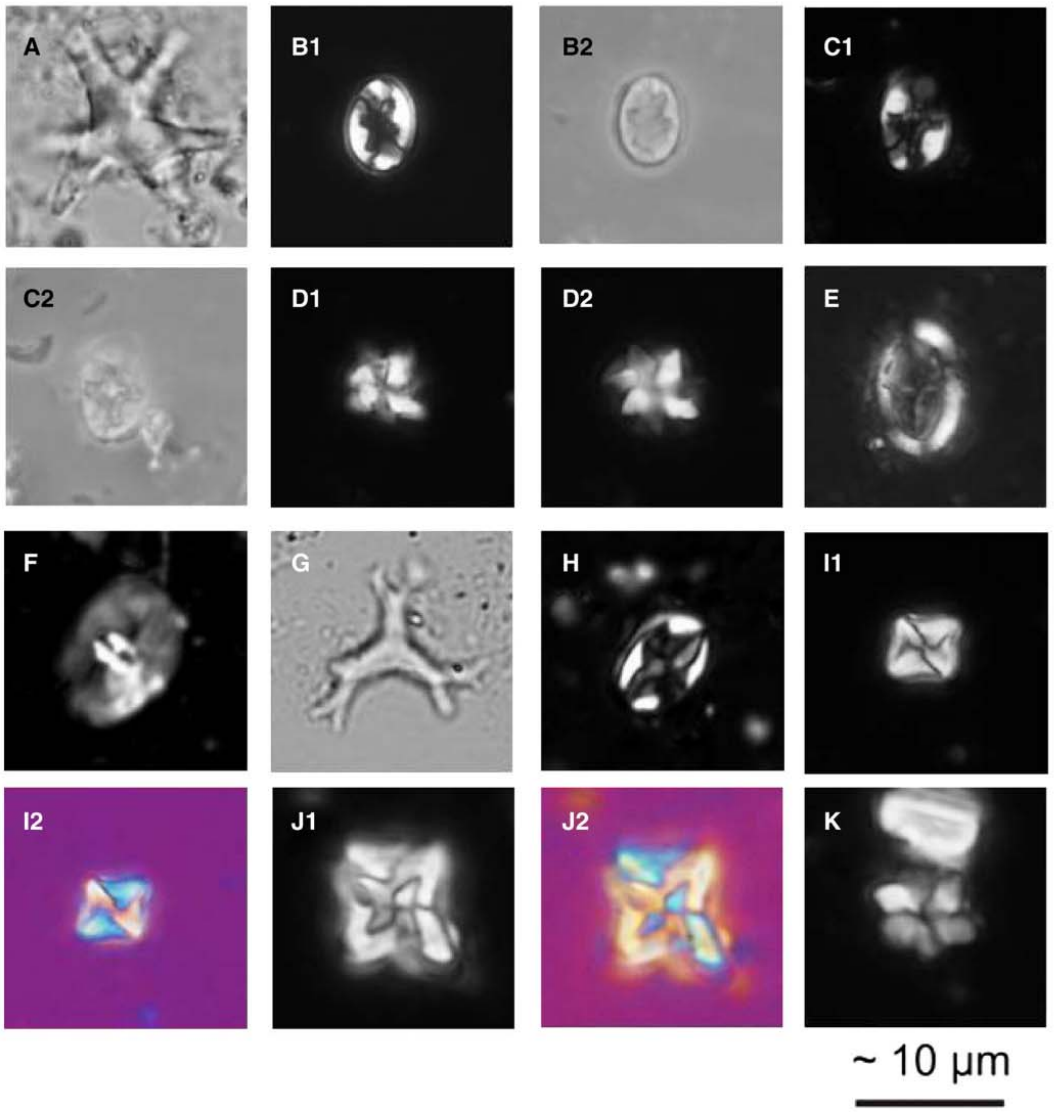

Plate 2. Light photomicrographs of select calcareous nannofossils from the Upper Turonian–Coniacian RASC optimum sequence at 1250× magnification. XPL = cross-polarized light. PL = plane light. PH = phase contrast. GYP = gypsum plate. A. *Liliasterites atlanticus*, U. Turonian, 47.24 m, Lozier Canyon, TX; PL. B. *E. perch-nielseniae*, Coniacian, 13.72 m, ACC #1, TX; B1: XPL, B2: PH. C. *E. eximius*, Coniacian, 13.72 m, ACC #1, TX; C1: XPL, C2: PH. D. *L. septenarius*, Coniacian, 13.72 m, ACC #1, TX; D1–2: XPL, high through low focus. E. *B. furtiva*, U. Turonian, 198 m, Mesa Verde, CO; XPL. F. *Zeugrhabdotus biperforatus*, Coniacian, miscellaneous drillcore, TX; XPL. G. *M. furcatus*, U. Turonian, 44.8 m, Lozier Canyon; TX; PL. H. *Helicolithus turonicus*, Turonian, miscellaneous drillcore, TX; XPL. I. *M. adumbrata*, Coniacian, 13.72 m, ACC #1, TX; I1: XPL, I2: GYP. J. *M. decussata*, U. Coniacian, 7.62 m, ACC #1, TX; J1: XPL, J2: GYP. K. *L. grillii*, U. Coniacian, 7.62 m, ACC #1, TX; XPL.

Above the low gamma Unnamed Member, ~75–120 m from the base of the Eagle Ford Formation, is another short (~5–10 m) high gamma facies. The HO of *E. moratus* and LO of *L. septenarius*, *Eiffellithus eximius* (Plate 2, Fig. C), and *Marthasterites* spp. occur within or at the top of this facies. This high gamma unit appears correlative to the Langtry Member at Lozier Canyon and South Bosque Shale in the ACC #1 core. The contact with a thick, lower gamma facies above this unit is the base of the Austin Chalk.

The LO of *M. decussata* occurs only ~7.5 m from the base of the Austin Chalk in the Saunders and Fasken cores at approximately the same level where the first *M. decussata* and *Micula* spp are found at Lozier Canyon and in the ACC #1. *Z. biperforatus* is only encountered in the Saunders

core more than 20 m above the base of the Austin Chalk along with *Micula concava*.

4.7. RASC

Ranked and scaled optimum sequences of calcareous nannofossil datums from the Cenomanian through Coniacian were calculated using the new data collected from the Western Interior combined with an additional 18 datasets from the literature (Table 1). The major events within carbon isotope records during OAE2 and the LO of inoceramid *C. d. erectus* were also incorporated into the analysis to provide placement of the Turonian and Coniacian stage boundaries, where possible. The ranked sequence of events, summarized in Table 2, shows the average position of each datum in relation to others and possible variations in their range. Using these range variations, which are highlighted in Table 2, it is also possible to interpret if pairs or groups of events are likely to be closely spaced or even coincident.

The scaled optimum sequence, shown in Table 3 and Fig. 7, uses the relative distance between datums in each dataset and reorders them with a cumulative distance value. Many taxa are in slightly different orders in the scaled versus the ranked sequence. This is a reflection of the rarity of many biostratigraphically important taxa, particularly at the end of their ranges. The averaging calculations of RASC give a statistically-based most likely placement of events. The scaled sequence should be viewed as a biostratigraphic framework of the averaged taxon ranges, and not necessarily the maximum observed extent. This can be used to judge the reliability of biostratigraphic datums compared to the ranked sequence and actual observations. A plot of the biostratigraphic horizons (Fig. 7) illustrates the placement of each datum based on the calculated distance between each event in the RASC optimum sequence.

5. Discussion

The sequence of events developed through analysis of 8 sites in the WIB reveals the limits of existing nannofossil zonation schemes. The ranges of several taxa are shortened in the optimum sequences as a result of the averaging methodology behind RASC calculations. This variability in the perceived stratigraphic placement of nannofossil datums cannot be completely explained by preservational effects or rare occurrences at the beginning/end of species ranges. A more critical analysis of the reliability of these datums in the CC and UC zonations, particularly in identifying OAE2 and the basal Coniacian, is possible using the Ranked and Scaled optimum sequence of events.

The events with the most observations and/or most reliably correlating to carbon isotope stratigraphy and macrofossil zonations are highlighted in the plot of biostratigraphic horizons (Fig. 7). Inconsistencies between the CC and UC zonations and the RASC optimum sequence are revealed when attempting to use many zonal markers. Key events in the excursion (first peak, second peak, base Turonian) and the LO of *C. d. erectus* are assumed to be fixed events for defining stage boundaries and the extent of OAE2. Closely spaced events on the horizontal axis represent closely spaced events in time.

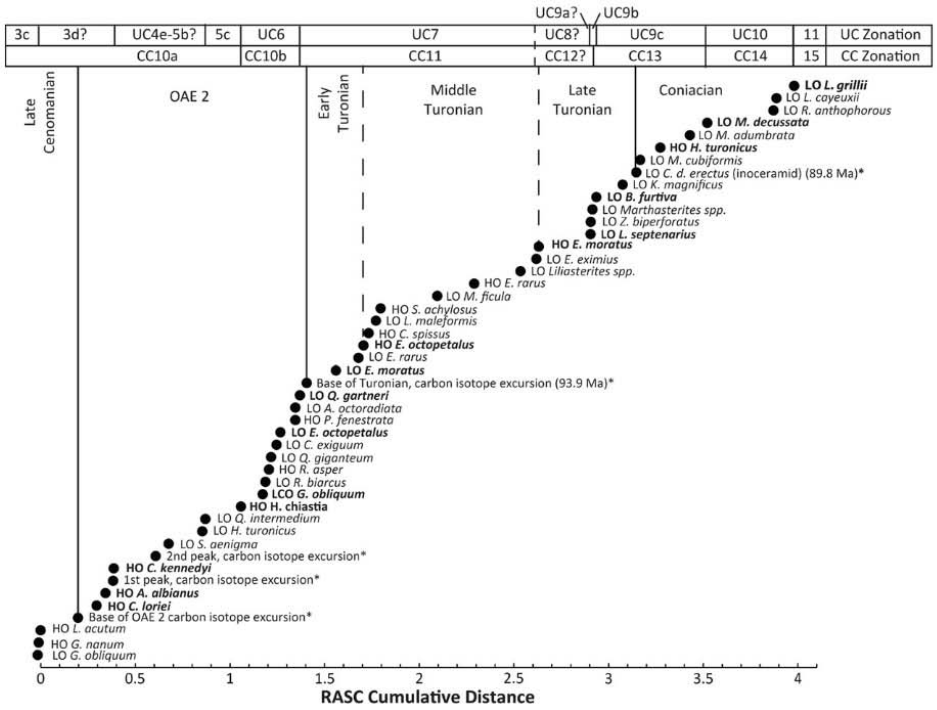

Fig. 7. A quantitatively derived optimum sequence of nannofossil biostratigraphic events from the Late Cenomanian to Coniacian, compared with interpreted boundaries in the CC (Perch-Nielsen, 1985) and UC (Burnett, 1998) zonations (Fig. 2). Events are equidistant on the vertical axis, while horizontal displacement reflects scaling on a relative time-scale determined through RASC statistical analysis of 26 datasets (refer to Agterberg and Gradstein, 1999). Events marked with (*) are supplementary datums with absolute ages (from Ogg and Hinnov, 2012), which allow for comparison to the geologic timescale. Nannofossil events in bold are interpreted as more reliable proxies for defining OAE2 and several stage/substage boundaries.

Groupings of events at the base of the Lower Turonian, Middle Turonian, Upper Turonian, and Coniacian indicate major evolutionary events or a concentration of datums onto major sequence boundaries/condensed sections. The group at the base of the Turonian consists of 11 events roughly equally divided between first and last occurrences. All 16 events within OAE2 are also nearly equally divided between speciations (9) and extinctions (7), suggesting significant turnover of calcareous nannofossils during this period. The species richness from samples in this study ranges from 80 to 90 taxa at Mesa Verde, indicating at least a 8–9% turnover rate. This is consistent with a comprehensive study of microfossil evolution through the middle Cretaceous by Leckie et al. (2002) which indicates 9% extinction and 6% speciation of calcareous nannofossils across the Cenomanian–Turonian boundary. In contrast, the group of 6 closely spaced events at the base of the Coniacian is mostly first occurrences. This suggests a diversification event at this boundary, although these biostratigraphic datums may also be closely spaced as a result of a major regression often associated with the Upper Turonian and basal Coniacian.

5.1. Lower and Middle Cenomanian biostratigraphy

Lower and Middle Cenomanian biostratigraphy is not discussed in detail because calcareous nannofossils found within this interval were too poorly preserved or the sections studied within the Western Interior contain only younger strata. The lowest samples collected from Mesa Verde, Rock Canyon, and Cuba are from the Upper Cenomanian in the central WIB. Revision of macrofossil zonations in west Texas by Cobban et al. (2008) indicate that the base of the Eagle Ford Formation (= Boquillas Formation) were deposited in the latter part of the Early Cenomanian, within ammonite zones *Forbesiceras brundrettei* and *Acompscoceras inconstans*. The LO of *C. kennedyi*, which should mark the base of Lower Cenomanian zones CC9c and UC1, occurs relatively high in the Eagle Ford Formation at Lozier Canyon and in the Saunders core, but this is due to the preservation in this part of the succession across Texas. *C. kennedyi* is found throughout the lower Eagle Ford Formation to within ~5–10 m of the contact with the Buda Limestone in the Fasken and Chamberlain cores. The ranges of *W. britannica* and *Z. xenotus*, recorded as a few rare occurrences in the unnamed shale member in the Fasken core and Cloice Member in the ACC #1 core, overlap with the base of *C. kennedyi* in the CC and UC zonations (Figs. 5, 6). This supports the local macrofossil interpretation from West Texas that the base of the Eagle Ford Formation is uppermost Lower Cenomanian.

5.2. Biostratigraphy of OAE2 and the Cenomanian–Turonian Boundary Interval

The highest occurrence of calcareous nannofossil *H. chiastia* and lowest occurrence of *Q. gartneri* are close to the Cenomanian–Turonian boundary and define the base and top, respectively, of zones CC10b and UC6 (Watkins, 1985; Tsikos et al., 2004; Kennedy et al., 2005). These two events are believed to straddle the top of the OAE2 carbon isotope excursion, which is used as a proxy for the base of the Turonian Stage at the GSSP in Rock Canyon near Pueblo, CO (Fig. 6; Tsikos et al., 2004; Kennedy et al., 2005). The highest occurrences of *A. albianus*, *C. kennedyi*, and lowest occurrences of *E. octopetalus* and *E. moratus* have also been shown to be useful through the interval defined by OAE2 (e.g. Bralower and Bergen, 1998; Fernando et al., 2010; Linnert et al., 2010, 2011a, 2011b). It should be noted that some authors use *Eprolithus eptapetalus*, which is a junior synonym of *E. moratus*. Additional nannofossil events occur within and around the interval of OAE2 and may prove useful with quantitative analysis. Integrated Upper Cenomanian through Lower Turonian biostratigraphy and carbon isotope chemostratigraphy from sites in the Western Interior and around the world (Bralower and Bergen, 1998; Hardas and Mutterlose, 2006; Tantawy, 2008; Fernando et al., 2010; Linnert et al., 2010, 2011a, 2011b) indicate several calcareous nannofossil datums that subdivide this interval that are not recognized in or conflict with established zonation schemes.

Comparing nannofossil biostratigraphy to carbon isotope chemostratigraphy in the Western Interior indicates the Cenomanian–Turonian boundary falls within zones CC10b and UC6. The HO of *H. chiastia* and LO of *Q. gartneri* have been shown to occur near the base of the Turonian and may even briefly overlap as is the case in the Amoco Rebecca Bounds core in western Kansas and at Eastbourne in the U.K. (Bralower and Bergen, 1998; Linnert et al., 2011a). In this case, CC10b and UC6 may be as little as ~56 kyrs in duration based on the results of Corbett and Watkins (2013) using the updated 2012 time scale (Ogg and Hinnov, 2012). Most of OAE2, a ~400–800 kyr event, would then be defined by a portion of subzone CC10a (Sageman et al., 2006; Voigt et al., 2008; Meyers et al., 2012). A plot of the cumulative distances between the RASC sequence of biostratigraphic events shows that the HO of *H. chiastia* occurs relatively close to the base of the Turonian, at 0.347 cumulative distance (Fig. 7, Table 3). Observations by Tsikos et al. (2004) show *Q. gartneri* to be a consistently accurate datum for the base of the Turonian stage and this is reflected in a small cumulative distance (0.036) between this boundary and the LO of *Q. gartneri*. These events are located close to the boundary in all but a few locations used in the WIB and therefore should be a reliable biostratigraphic marker regionally.

Where *H. chiastia* and *Q. gartneri* are rare, the presence of other calcareous nannofossil events can be more dependable biostratigraphic markers. Several biostratigraphic datums fall in a short interval in the gap zone between these two taxa in the scaled optimum sequence, indicating a significant turnover of calcareous nannofossil species during OAE2 (Table 3, Fig. 7). The appearance of *E. octopetalus* and *E. moratus* also approximate the Cenomanian–Turonian boundary, and first occur just below the boundary and above the HO of *C. kennedyi* and *A. albianus*. They are not recognized in the CC zonation, but are secondary markers in UC zones 5–6. Where even these taxa are rare, in the southern Western Interior, the lowest common occurrence (LCO) of *G. obliquum* may serve as a more reliable datum for the base of the Turonian (Figs. 5, 6).

The HO of *C. kennedyi* and *Lithraphidites acutum* Verbeek and Manivit (Plate 1, Fig. A) marks the base of Upper Cenomanian subzones CC9c and CC10a. Variability in the HO of *L. acutum* and *A. albianus* and LO of *Rotelapillus biarcus* (Plate 1, Fig. K) makes the use of zones UC3e-5a difficult in many sections. *L. acutum* is a delicate form that is often destroyed by diagenesis, making this species less reliable as a biostratigraphic marker. On the other hand, *C. kennedyi* is a robust nannofossil resistant to diagenesis that goes extinct in the earlier stages of OAE2. Equally resistant are *C. loriei* (*Cretarhabdus striatus* of some authors) and *A. albianus*, the HO of which can be used as alternative markers. *C. kennedyi* and *A. albianus* occur higher in sections (B interval of OAE2) from the KWIS than elsewhere (near the basal A interval of OAE2), and since they are more resistant forms they may be reworked here. While bioturbation is reported in sediments from this interval at Pueblo (Kennedy et al., 2005) it is difficult to prove reworking versus a diachronous extinction. The rarity and significant differences between the RASC optimum sequences and many observations limit use of *R. asper*, *Staurolithites aenigma* Burnett (Plate 1, Fig. E), *R. biarcus* and *Quadrum intermedium* Varol (Plate 1, Fig. F) as high resolution markers. The LO of *H. turonicus*, *A. octoradiata* and *Quadrum giganteum* Varol (Plate 1, Fig. Q) is also recognized in too few locations to be used as dependable biostratigraphic datums.

5.3. Turonian biostratigraphy

Historically the LO of *E. eximius* has been used to mark the boundary between the lower and middle Turonian at the base of CC12 and UC8. The emended species concepts by Shamrock and Watkins (2009) separate earlier Turonian morphotypes with slightly off-axis crosses into the

species *Eiffellithus perch-nielseniae* (Plate 2, Fig. B). The morphotype of *E. eximius* with a nearly perfectly straight axial cross (Plate 2, Fig. C) is only recognized at or above the LO of upper Turonian taxa in this study. The HO of *E. octopetalus* may be a possible proxy for the top of the Lower Turonian in nannofossil zonations (Varol, 1992; Linnert et al., 2010; Corbett and Watkins, 2013, in pressa, in pressb). This event appears to approximately coincide with the boundary based on comparisons with macrofossil zonations recorded at Mesa Verde, CO and correlated to the Wunstorf Core in Germany (Leckie et al., 1997; Linnert et al., 2010; Corbett and Watkins, 2013, in pressa). The LO of the genus *Liliasterites* was proposed by Watkins et al. (1998) to subdivide Upper Turonian zone CC12 and occurs only in the Upper Turonian and Lower Coniacian. There is a relatively large cumulative distance in the RASC sequence of events between *E. octopetalus* and *Liliasterites* which supports these interpretations. These taxa may be useful to approximate the Turonian substages in addition to well established zonal markers.

Several older zonation schemes including the CC zonation of Perch-Nielsen (1985) rely on the first occurrence of *M. furcatus* to approximate Turonian–Coniacian boundary (at the base of subzone CC13a; Fig. 2). The LO of *L. septenarius* defined subzone CC13b, but Corbett and Watkins (in pressb) document the first occurrence of this species well below that of *M. furcatus*. *M. furcatus* and *L. septenarius* first occur above erosional surfaces at the base of the Niobrara in Colorado and Kansas (Bralower and Bergen, 1998). These events, as well as the LO of *E. eximius*, occur within the transgressive Langtry Member just below the Austin Chalk in the more distal expanded sections in Webb Co., TX and at Lozier Canyon on the carbonate platform (Figs. 1, 4A, 5). In the Austin area, which would have been more exposed during this period (Fig. 1), these events occur in a condensed transgressive lag at the base of the Austin Chalk. These observations are consistent with the earlier work of Smith (1981) and Jiang (1989) from numerous localities of the Eagle Ford and Austin contacts across Texas. The contact at the bases of the Langtry Member and Niobrara Formation represents an unconformity which formed during a major late Turonian regression within the Western Interior Seaway (Hattin, 1975b; Laferriere, 1987; Walaszczyk and Cobban, 2000; Walaszczyk et al., 2012). The inoceramid *C. d. erectus* is widespread and found consistently above this surface, indicating that nannofossil zones CC13 and UC9 have their bases in the Upper Turonian.

Jiang (1989) also noted that the LO of *M. furcatus* and *L. septenarius* is coincident with the Upper Turonian ammonite *Prionocyclus* in the uppermost Eagle Ford and suggested the HO of *E. moratus* at the base of the Austin Chalk as more accurate Coniacian boundary criteria. The HO of *E. moratus* is found just below the base of the Niobrara in the Rebecca Bounds core and in an interval from the Langtry Member to basal Austin Chalk across Texas. This is below the observed LO of *C. d. erectus* and coincides with the base of zones CC13 and UC9. In the absence of other key taxa this event could provide a reliable marker for the base of the Upper Turonian, as opposed to the Coniacian.

5.4. Biostratigraphy of the Turonian–Coniacian Boundary Interval

Historically the base of the Niobrara Formation and Austin Chalk marked the boundary between the Turonian and Coniacian stages in the WIB (e.g., Freeman, 1961; Pessagno, 1967; Kauffman, 1977; Laferriere, 1987). Recent attempts to revise the base of the Coniacian stage, using the first occurrence of inoceramid *C. d. erectus*, have likely changed the placement of this boundary (Kauffman et al., 1996; Ogg et al., 2004; Ogg and Hinnov, 2012).

A comprehensive review of macrofossil biostratigraphy and investigation of key localities across the Western Interior by Walaszczyk and Cobban (2000) reveal the base of the Niobrara Formation and associated facies/members are time transgressive from north–south. The Fort Hays Member at the base of the Niobrara Formation is Upper Turonian at Wagon Mound and Springer, NM but gets progressively younger to the north (Laferriere, 1987; Walaszczyk and Cobban, 2000; Walaszczyk et al., 2012). Macrofossil correlations by Fisher et al. (1985) and Collum (1990) reveal that the LO of *Inoceramus/Cremnoceramus rotundatus* (= *C. d. erectus*) is found several meters up in the middle of the Fort Hays Member across Colorado and Kansas and the Fort Hays is entirely Coniacian in South Dakota (Walaszczyk and Cobban, 2000). The occurrence of *C. d. erectus* with respect to the base of the Fort Hays reflects gradual transgression and deposition of the Niobrara over the mid–late Turonian unconformity (Walaszczyk and Cobban, 2000; Walaszczyk et al., 2012).

Only a few observations have been made of *C. d. erectus* in the southern Western Interior. Cobban et al. (2008) note the LO of *C. d. erectus* at the top of the Ernst Member of the Boquillas Formation in Big Bend National Park and *Cremnoceramus* sp. approximately 23 m above the base near Lozier Canyon in Texas. Larson et al. (1997) and Hancock and Walaszczyk (2004) show the *C. d. erectus* zone ~0.5 m above the base of the Austin Chalk in and around Dallas, TX. They suggest that the thin and missing macrofossil zones in the basal Austin and underlying Eagle Ford also reflect a condensed succession overlying an Upper Turonian unconformity.

Coquand's (1857a, 1857b) original Coniacian boundary in France was marked by the first occurrence of ammonite *Forresteria* (*Harleites*) *petrocoriensis* Coquand (Birkelund et al., 1984). The Brussels meeting of the Coniacian Working Group of the Cretaceous Subcommission on Stratigraphy (Kauffman et al., 1996) interpreted the LO of *C. d. erectus* to co-occur with that of *F.* (*H.*) *petrocoriensis* and other basal Coniacian markers in Europe, making a suitable replacement especially where *F.* (*H.*) *petrocoriensis* is absent in the Western Interior (e.g., Larson et al., 1997; Walaszczyk and Cobban, 2000). The latest revisions to the geologic timescale show these events not to be coincident as the LO of *C. d. erectus* occurs above that of *F.* (*H.*) *petrocoriensis* (Walaszczyk and Cobban, 2000; Kennedy and Walaszczyk, 2004; Ogg and Hinnov, 2012). This implies the boundary should be found at a stratigraphically and temporally higher level with respect to existing calcareous nannofossil zonations.

Lees (2008) made the first attempts to create a revised nannofossil biostratigraphic framework for the basal Coniacian based largely on analysis of two proposed GSSPs in Europe: the Salzgitter–Salder quarry in Germany and Slupia Nadbrzezna in Poland. The lowest occurrences of a form identified as *Broinsonia parca expansa* (herin considered to be *B. furtiva*) and *M. decussata*, which define subzone UC9c, bracket the lowest occurrence of *C. d. erectus* at candidate GSSP sites.

The only large species of *Broinsonia* observed in Lower Coniacian strata in this study does not resemble the original description and figures of *B. parca* subs *expansa* (see Wise, 1983) and more closely resemble *B. furtiva* (Bukry) Hattner, Wind and Wise (Plate 2, Fig. E; Hattner and Wise, 1980). While the sizes of the type specimens overlap, the pores appear larger and can occur along the edge of the rim in *B. p.* subs *expansa*, whereas the pores of *B. furtiva* only occur along the axial sutures within the central plate. *B. furtiva* is therefore used in place of *B. parca expansa*. Significant taxonomic work is still required to determine the precise evolutionary divergence of these two taxa, which must be above the stratigraphic interval analyzed in this study.

The lowest occurrence of *M. adumbrata* and highest occurrence of *H. turonicus* can provide greater precision to approximate the location of the Coniacian boundary (Lees, 2008). The LO of *L. septenarius*, *M. furcatus*, *Z. biperforatus*, and *B. furtiva* occurs below the LO of *C. d. erectus* at all the sites investigated by Lees and below *F.* (*H.*) *petrocoriensis* at Slupia Nadbrzezna, suggesting an Upper Turonian age. The LO of *M. decussata* and LO of *B. furtiva* bracket the LO of *C. d. erectus* and limit the base of the Coniacian to within UC subzone 9c. The LO of *M. adumbrata* and *H. turonicus* successively constrains the placement of the boundary to narrow interval in this zone.

The sequence of events from the Upper Turonian through Lower Coniacian recognized by Lees (2008) and Walaszczyk et al. (2012)

is consistently reproduced across the WIB. At the proposed GSSPs, *M. furcatus* and *L. septenarius* occur well below the LO of *C. d. erectus*. Their placement, as well as the HO of *E. moratus*, should be revised to reflect an Upper Turonian appearance (Sikora et al., 2004; Lees, 2008). *B. furtiva* and *Z. biperforatus* are very rare in the sections across Texas, although *B. furtiva* is first observed less than 10 m above the base of the Austin in West Texas and in the condensed interval with *M. furcatus* and *L. septenarius*. The LO of *M. decussata* is observed consistently ~7–10 m above the base of the Austin Chalk in Webb Co. and in the ACC #1 core and *Micula* spp. occur ~10 m above the base along Hwy 90. Jiang (1989) also documented this event 7.5 m above the base of the Austin near Dallas, TX. In the ACC #1 core the HO of *H. turonicus* and LO of *M. adumbrata* show that this boundary likely occurs in the lower 6 m of Austin Chalk. The implies a placement of the Coniacian stage boundary in the lower 10 m of the Austin Chalk in the southern Western Interior, and while observations of *C. d. erectus* are scarce, this is consistent with analysis of Dallas area outcrops by Larson et al. (1997) and Hancock and Walaszczyk (2004). Quantitative analysis of these nannofossil events provides a RASC optimum sequence comparable to that observed by Lees (2008; Fig. 7). The HO of *H. turonicus* and LO of *B. furtiva* are the closest events to the LO of *C. d. erectus*, while the HO of *M. decussata* can be used to define a larger stratigraphic interval approximating the Coniacian boundary.

Significant differences between the CC and UC nannofossil zonation schemes and the 2008 and 2012 revisions to the geologic timescale indicate problems correlating microfossil datums to the redefined definition of the Coniacian stage boundary (Ogg et al., 2004; Sikora et al., 2004; Ogg et al., 2008; Donovan et al., 2012; Ogg and Hinnov, 2012; Walaszczyk et al., 2012). Consistent recognition of the sequence of events generated from the candidate GSSPs across the Western Interior suggests that the base of the Coniacian boundary can be approximately identified with calcareous nannofossils even in the absence of the primary marker *C. d. erectus*.

6. Conclusions

A qualitative and quantitative analysis of calcareous nannofossils of samples from Colorado, Kansas, and Texas has resulted in the development of an idealized sequence of biostratigraphic events for the Upper Cenomanian through Coniacian deposits of the central and southern WIB. Combined with available published data a comparison can be made to well established global zonation schemes. Using new observations from 8 localities in this study and RASC analysis of a global dataset of 26 sites we suggest priority be given to 15 calcareous nannofossil datums that are most reliable for distinguishing some of the major stage and substage boundaries from the Upper Cenomanian through Coniacian (Fig. 7). The cosmopolitan CC zonation of Perch-Nielsen (1985) (Fig. 2) remains an accurate framework, but is not detailed enough to subdivide successions on the scale of hundreds of thousands of years (Fig. 7). The UC zonation developed by Burnett (1998) utilizes more events and provides at a higher resolution across this time interval (Fig. 2). While the UC zonation appears reliable for approximating the placement of the base of the Coniacian stage in the absence of the inoceramid *C. d. erectus* many subzones in the upper Cenomanian through middle Turonian cannot be used (Fig. 7). Some species concepts are different from current interpretations (e.g., *E. eximius*, *B. furtiva*) while observations and quantitative analysis of calcareous nannofossil events reveal an optimum sequence of events inconsistent with the placement of subzonal markers during this interval. Despite these observations, and without any explanation, the 2012 revisions to the geologic timescale make adjustments to the placement of calcareous nannofossil zones and biostratigraphic datums. The RASC optimum sequence is an attempt at a more accurate placement of events within the new timescale.

Supplementary data related to this article can be found online at http://dx.doi.org/10.1016/j.marmicro.2014.04.002.

Acknowledgments

This study was completed in partial fulfillment of a PhD dissertation and supported by a research assistantship with the North America Gas Division of BP America and the University of Nebraska–Lincoln as well as the Gulf Coast Section of SEPM Ed Picou Fellowship and American Association of Petroleum Geologists Rodney A. Bernasek Memorial Grant. We would like to thank Scott Staerker and Art Donovan for their financial support and advice and access to the BP-leased Eagle Ford Field Laboratory at Lozier Canyon, TX, permission to use proprietary data, and providing helpful discussion, as well as Swift Energy for their permission to use the Chamberlain drillcore and Fasken well data. We are also very thankful for the assistance of Stephen Ruppel and James Donnelly and the permission of the Bureau of Economic Geology at the University of Texas at Austin for sampling of the ACC #1 core. We would also like to thank R. Mark Leckie for providing samples of his collection from Mesa Verde National Park, CO. Thanks also go to Chris Lowery for his partnership in the field and insights into the analysis of Lozier Canyon, the Fasken core, and ACC #1 core.

Appendix A

Ahmuellerella octoradiata (Górka) Reinhardt and Górka 1967
Axopodorhabdus albianus (Black) Wind and Wise 1977
Broinsonia furtiva (Bukry) Hattner Wind and Wise 1980
Broinsonia parca subsp. expansa (Stradner) Wise and Watkins 1983
Chiastozygus spissus Bergen 1998
Corollithion exiguum Stradner 1961
Corollithion kennedyi Crux 1981
Cretarhabdus loriei Gartner 1968
Eiffellithus eximius (Stover) Perch-Nielsen 1968
Eiffellithus nudus Shamrock 2009
Eiffellithus perch-nielseniae Shamrock 2009
Eprolithus floralis (Stradner) Stover 1966
Eprolithus moratus (Stover) Burnett, 1998
Eprolithus octopetalus Varol, 1992
Eprolithis rarus Varol, 1992
Gartnerago costatum costatum (Bukry) Forchheimer 1972
Gartnerago obliquum (Stradner) Nöel 1970
Gartnerago nanum Thierstein 1974
Helenia chiastia Worsley 1971
Helicolithus turonicus Varol and Girgis 1994
Kamptnerius magnificus Deflandre 1959
Liliasterites spp. Stradner and Steinmetz 1984
Lithraphidites acutum Verbeek and Manivit 1977
Lithatrinus grillii Stradner 1962
Lithastrinus septenarius Forchheimer 1972
Lucianorhabdus cayeuxii Deflandre 1959
Lucianorhabdus maleformis Reinhardt 1966
Marthasterites furcatus Deflandre 1959
Micula adumbrata Burnett 1997
Micula decussata (= *M. staurophora*) Vekshina 1959
Micula concava (Stradner) Verbeek 1976
Micula cubiformis Forchheimer 1972
Miravetsina ficula (Stover) Bergen 1998
Percivalia fenestrata (Worsley) Wise, 1983
Quadrum gartneri Prins and Perch-Nielsen 1977
Quadrum giganteum Varol, 1992
Quadrum intermedium Varol, 1992
Quadrum svabenickae Burnett 1997
Reinhardtites anthophorus (Deflandre) Perch-Nielsen 1968
Rhagodiscus asper (Stradner) Reinhardt 1967
Rotelapillus biarcus (Bukry) Lees and Bown, 2005
Staurolithites aenigma Burnett 1997
Stoverius achylosus (Stover) Perch-Nielsen 1986

Watznaueria britannica (Stradner) Reinhardt 1964
Zeugrhabdotus biperforatus (Gartner) Burnett 1997
Zeugrhabdotus xenotus (Stover) Burnett 1996

Appendix B

Complete spreadsheet of events from all 26 localities can be found at the World Data Center-A, http://www.ncdc.noaa.gov/paleo/data.html (Corbett et al., submitted for publication).

Appendix C

A more detailed description of the localities from which new data is presented can be found in the online supplementary materials.

References

Agterberg, F.P., Gradstein, F.M., 1999. The RASC method for ranking and scaling of biostratigraphic events. Earth Sci. Rev. 46, 1–25.

Arthur, M.A., Dean, W.A., Pratt, L.M., 1988. Geochemical and climatic effects of increased marine organic burial at the Cenomanian/Turonian boundary. Nature 335, 714–717.

Birkelund, T., Hancock, J.M., Hart, M.B., Rawson, P.F., Remane, J., Robaszynski, R., Schmid, F., Surlyk, F., 1984. Cretaceous stage boundaries — proposals. Geol. Soc. Den. Bull. 33, 3–20.

Blakey, R., 2012. Paleogeography of Western North America. Colorado Plateau Geosystems, Inc.(DVD).

Bowman, A.R., Bralower, T.J., 2005. Paleoceanographic significance of high-resolution carbon isotope records across the Cenomanian–Turonian boundary in the Western Interior and New Jersey coastal plain, USA. Mar. Geol. 217, 305–321.

Bralower, T.J., 1988. Calcareous nannofossil biostratigraphy and assemblages of the Cenomanian–Turonian boundary interval: implications for the origin and timing of oceanic anoxia. Paleoceanography 3 (3), 275–316.

Bralower, T.J., Bergen, J.A., 1998. Cenomanian–Santonian calcareous nannofossil biostratigraphy of a transect of cores drilled across the Western Interior Seaway. In: Dean, W.E., Arthur, M.A. (Eds.), Stratigraphy and paleoenvironments of the Cretaceous Western Interior Seaway. USA. SEPM Concepts in Sedimentology and Paleontology No. 6, pp. 101–126.

Burnett, J.A. (with contributions from Gallagher, L.T. and Hampton, M.J.), 1998. Upper Cretaceous. In: Bown, P.R., (Ed.) Calcareous Nannofossil Biostratigraphy, British Micropalaeontological Society Publications Series. London: Chapman and Hall/Kluwer Academic Publishers, pp. 132–199.

Burns, C.E., Bralower, T.J., 1998. Upper Cretaceous nannofossil assemblages across the Western Interior Seaway: implications for the origins of lithologic cycles in the Greenhorn and Niobrara Formations. In: Dean, W.E., Arthur, M.A. (Eds.), Stratigraphy and paleoenvironments of the Cretaceous Western Interior Seaway. USA. SEPM Concepts in Sedimentology and Paleontology No. 6, pp. 101–126.

Cobban, W.A., Hook, S.C., McKinney, K.C., 2008. Upper Cretaceous molluscan record along a transect from Virden, New Mexico, to Del Rio, Texas. N. M. Geol. 30 (3), 75–92.

Collum, C.J., 1990. High-resolution Stratigraphic and Paleoenvironmental Analysis of the Turonian–Coniacian stage boundary interval (Late Cretaceous) in the Lower Fort Hays Limestone Member, Niobrara Formation, Colorado and New Mexico. (Thesis) Brigham Young University.

Coquand, H., 1857a. Notice sur la formation crétacée du département de la Charente. Bull. Soc. Geol. Fr. Série 2 (14), 55–98.

Coquand, H., 1857b. Position des Ostrea columba et biauriculata dans le groupe de la craie inférieure. Bull. Soc. Geol. Fr. Série 2 (14), 745–766.

Corbett, M.J., Watkins, D.K., 2013. Calcareous nannofossil paleoecology of the mid-Cretaceous Western Interior Seaway and evidence of oligotrophic surface waters during OAE2. Palaeogeogr. Palaeoclimatol. Palaeoecol. 392, 510–523.

Corbett, M.J., Watkins, D.K., 2014a. Cenomanian through Basal Coniacian Calcareous Nannofossil Biostratigraphy of the Mancos Shale Reference Section, Mesa Verde, CO (in press).

Corbett, M.J., Watkins, D.K., 2014b. Transitional forms in the Eprolithus–Lithastrinus lineage. Micropaleontology (in press).

Corbett, M.J., Lowery, C.M., Miceli Romero, A., Watkins, D.K., Leckie, M.R., Li, W., Pramudito, A., Donovan, A., Staerker, S., 2011. A bio-chemostratigraphic framework of Oceanic Anoxic Event 2 at Lozier Canyon, TX: correlations to the Western Interior Seaway and comparison to sequence stratigraphic surfaces. GSA Abstr. Programs 43 (5), 611.

Corbett, M.J., Watkins, D.K., Pospichal, J.J., 2014. World Data Center-A. http://www.ncdc.noaa.gov/paleo/data.html (Boulder, Colorado, submitted for publication).

Desmares, D., Grosheny, D., Beaudoin, B., Gardin, S., Gauthier-Lafaye, F., 2007. High resolution stratigraphic record constrained by volcanic ash beds at the Cenomanian–Turonian boundary in the Western Interior Basin, USA. Cretac. Res. 28, 561–582.

Donovan, A.D., Staerker, T.S., Pramudito, A., Weiguo, L., Corbett, M.J., Lowery, C.M., Miceli Romero, A., Gardner, R., 2012. The Eagle Ford outcrops of West Texas: a laboratory for understanding heterogeneities within unconventional mudstone reservoirs. GCAGS J. 1, 162–185.

Elder, W.P., 1985. Biotic patterns across the Cenomanian–Turonian extinction boundary near Pueblo, CO. In: Pratt, L.M., Kauffman, E.G., Zelt, F.B. (Eds.), Fine-grained Deposits and Biofacies of the Cretaceous Western Interior Seaway: Evidence of Cyclic Sedimentary Processes: SEPM Field Trip Guidebook No. 4, pp. 157–169.

Eleson, J.W., Bralower, T.J., 2005. Evidence of changes in the surface water temperature and productivity at the Cenomanian/Turonian boundary. Micropaleontology 51 (4), 319–332.

Fairbanks, M.D., Ruppel, S.C., 2012. High resolution stratigraphy and facies architecture of the Upper Cretaceous (Cenomanian–Turonian) Eagle Ford Formation, Central Texas. AAPG Search and Discovery Article (Article # 10408).

Fernando, A.G.S., Takashima, R., Nishi, H., Giraud, F., Okada, H., 2010. Calcareous nannofossil biostratigraphy of the Thomel Level (OAE2) in the Lambruisse section, Vocotian Basin, southeast France. Geobios 43, 45–57.

Fisher, A.G., Herbert, T., Premoli-Silva, I., 1985. Carbonate bedding cycles in Cretaceous pelagic and hemipelagic sediments. In: Pratt, L.M., Kauffman, E.G., Zelt, F.B. (Eds.), Fine-grained deposits and biofacies of the Cretaceous Western Interior Seaway: evidence of cyclic sedimentary processes. SEPM Field Trip Guidebook, vol. 4, pp. 1–10.

Freeman, V.L., 1961. Contact of the Boquillas flags and Austin Chalk in Val Verde, Terrell, and Brewster counties, Texas. U.S. Geol. Soc. Prof. Pap. 594-K.

Geisen, M., Bollman, J., Herrle, J.O., Mutterlose, J., Young, J.R., 1999. Calibration of the random settling technique for calculation of absolute abundances of calcareous nannoplankton. Micropaleontology 45, 437–442.

Gradstein, F.M., Agterberg, F.P., Brower, J.C., Schwarzacher, W.S. (Eds.), 1985. Quantitative Stratigraphy. Unesco, France.

Hammer, Ø., Harper, D., 2006. Paleontological Data Analysis. Blackwell Publishing, Malden, MA.

Hancock, J.M., Walaszczyk, I., 2004. Mid-Turonian to Coniacian changes of sea level around Dallas, Texas. Cretac. Res. 25, 459–471.

Hardas, P., Mutterlose, J., 2006. Calcareous nannofossil biostratigraphy of the Cenomanian/Turonian boundary interval of ODP Leg 207 at the Demerara Rise. Rev. Micropaleontol. 49, 165–179.

Hattin, D.E., 1975a. Stratigraphy and depositional environment of Greenhorn Limestone (Upper Cretaceous) of Kansas. Kans. Geol. Surv. Bull. 209.

Hattin, D.E., 1975b. Stratigraphic study of the Carlile–Niobrara (Upper Cretaceous) unconformity in Kansas and northeastern Nebraska. In: Caldwell, W.G.E. (Ed.), The Cretaceous system in the Western Interior of North America. Geological Association of Canada, Special Paper, 13, pp. 195–210.

Hattner, J.G., Wise, S.W., 1980. Upper Cretaceous calcareous nannofossil biostratigraphy of South Carolina. S. C. Geol. 24 (2), 41–117.

Jarvis, I., Gale, A.S., Jenkyns, H.C., Pearce, M.A., 2006. Secular variation in Late Cretaceous carbon isotopes: a new ^{13}C carbonate reference curve for the Cenomanian–Campanian (99.6–70.6 Ma). Geol. Mag. 143 (5), 561–608.

Jiang, M.-J., 1989. Biostratigraphy and Geochronology of the Eagle Ford shale, Austin Chalk, and Lower Taylor Marl in Texas Based on Calcareous Nannofossils. (Dissertation) , vols. I and II. Texas A&M University.

Kauffman, E.G., 1977. Geological and biological overview: Western Interior Cretaceous Basin. Mt. Geol. 14 (3–4), 75–99.

Kauffman, E.G., Caldwell, W.G.E., 1994. (mis-dated 1993). The Western Interior Basin in space and time. In: Caldwell, W.G.E., Kauffman, E.G. (Eds.), Evolution of the Western Interior Basin. Geological Association of Canada, Special Paper, 39, pp. 1–30.

Kauffman, E.G., Kennedy, W.J., Wood, C.J., 1996. The Coniacian stage and substage boundaries. Bull. Inst. R. Sci. Nat. Belg. Sci. Terre 66, 81–94 (Supplement).

Kemple, W.G., Sadler, P.M., Strauss, D.J., 1995. Extending graphic correlation to many dimensions: stratigraphic correlation as constrained optimization. In: Mann, K.O., Lane, H.R. (Eds.), Graphic correlation. SEPM Special Publication No. 53, pp. 65–82.

Kennedy, W.J., Walaszczyk, I., 2004. *Forresteria* (*Harleites*) *petrocoriensis* (Coquand, 1859) from the Upper Turonian *Mytiloides scupini* Zone of S upia Nadbrze na, Poland. Acta Geol. Pol. 54, 55–59.

Kennedy, W.J., Walaszczyk, I., Cobban, W.A., 2005. The global boundary stratotype section and point for the base of the Turonian Stage of the Cretaceous: Pueblo, Colorado, U.S.A Episodes 28 (2), 93–104.

Laferriere, A.P., 1987. Cyclic sedimentation in the Fort Hays Limestone Member, Niobrara Formation (Upper Cretaceous) in Northeastern New Mexico and Southeastern Colorado. New Mexico Geological Society Guidebook, 38th Field Conference, Northeastern New Mexico, pp. 249–254.

Larson, P.A., Morin, R.W., Kauffman, E.G., Larson, A., 1997. Sequence stratigraphy and cyclicity of Lower Austin/Upper Eagle Ford Outcrops (Turonian–Coniacian), Dallas County, Texas. Dallas Geol. Soc. Field Trip 5.

Leckie, R.M., Kirkland, J.I., Elder, W.P., 1997. Stratigraphic framework and correlation of a principal reference section of the Mancos Shale (Upper Cretaceous), Mesa Verde, Colorado. New Mexico Geological Society Guidebook, 48th Field Conference, Mesozoic Geology and Paleontology of the Four Corners Region, pp. 163–216.

Leckie, R.M., Yuretich, R.F., West, O.L.O., Finkelstein, D., Schmidt, M., 1998. Paleoceanography of the Southwestern Western Interior Sea during the time of the Cenomanian–Turonian boundary (Late Cretaceous). In: Dean, W.E., Arthur, M.A. (Eds.), Stratigraphy and paleoenvironments of the Cretaceous Western Interior Seaway, USA. SEPM Concepts in Sedimentology and Paleontology No. 6, pp. 101–126.

Leckie, R.M., Bralower, T.J., Cashman, R., 2002. Oceanic anoxic events and plankton evolution: biotic response to tectonic forcing during the mid-Cretaceous. Paleoceanography 17 (3), 1–29.

Lees, J.A., 2008. The Calcareous nannofossil record across the Late Cretaceous Turonian/Coniacian boundary, including new data from Germany, Poland, the Czech Republic and England. Cretac. Res. 29, 40–64.

Lees, J.A., Bown, P.R., 2005. Upper Cretaceous calcareous nannofossil biostratigraphy, ODP Leg 198 (Shatsky Rise, Northwest Pacific Ocean). In: Bralower, T.J., Premoli Silva, I., Malone, M.J. (Eds.), Proceedings of the Ocean Drilling Program, Scientific Results, 198, pp. 1–60.

Linnert, C., Mutterlose, J., Erbacher, J., 2010. Calcareous nannofossils of the Cenomanian/Turonian boundary interval from the Boreal Realm (Wunstorf, northwest Germany). Mar. Micropaleontol. 74, 38–58.

Linnert, C., Mutterlose, J., Mortimore, R., 2011a. Calcareous nannofossils from Eastbourne (Southeastern England) and the paleoceanography of the Cenomanian–Turonian boundary interval. Palaios 26, 298–313.
Linnert, C., Mutterlose, J., Herrle, J.O., 2011b. Late Cretaceous (Cenomanian–Maastrichtian) calcareous nannofossils from Goban Spur (DSDP Sites 549, 551): implications for the palaeoceanography of the proto North Atlantic. Palaeogeogr. Palaeoclimatol. Palaeoecol. 299, 507–528.
Lowery, C.M., Corbett, M.J., Leckie, R.M., Watkins, D.K., Staerker, T.S., Donovan, A., 2014. Foraminiferal Evidence of Paleoceanographic Transitions in the Cenomanian–Turonian Eagle Ford Shale across Southern Texas (in review).
Meyers, S.R., Sageman, B.B., Arthur, M.A., 2012. Obliquity forcing of organic matter accumulation during Oceanic Anoxic Event 2. Paleoceanography 27, PA3212.
Ogg, J.G., Hinnov, L.A. (contributions by C. Huang), 2012. Cretaceous. In: Gradstein, F.M., Ogg, J.G., Schmitz, M., and Ogg, G., (Eds.) The Geologic Time Scale 2012. Elsevier, Amsterdam.
Ogg, J., Lugowski, A., 2013. TSCreator Visualization of Enhanced Geologic Time Scale 2012 Database (Version 6.1; 2013). (http://www.tscreator.org).
Ogg, J.G., Agterberg, F.P., Gradstein, F.M., 2004. The Cretaceous Period. In: Gradstein, F.M., Ogg, J.G., Smith, A.G. (Eds.), A Geologic Time Scale 2004. Cambridge University Press, Cambridge, pp. 344–383.
Ogg, J.G., Ogg, G., Gradstein, F.M., 2008. The Concise Geologic Time Scale. Cambridge University Press, Cambridge (184 pp.).
Perch-Nielsen, K., 1985. Mesozoic calcareous nannofossils. In: Bolli, H.M., Saunders, J.B., Perch-Nielsen, K. (Eds.), Plankton Stratigraphy, 1, pp. 329–426.
Pessagno, E.A., 1967. Upper Cretaceous foraminifera from the Western Gulf Coastal Plain. Paleontogr. Am.z 5 (37), 245–445.
Pratt, L.M., 1985. Isotopic studies of organic matter and carbonate in rocks of the Greenhorn marine cycle. In: Pratt, L.M., Kauffman, E.G., Zelt, F.B. (Eds.), Fine-grained Deposits and Biofacies of the Cretaceous Western Interior Seaway: Evidence of Cyclic Sedimentary Processes: SEPM Field Trip Guidebook No. 4, pp. 151–156.
Sageman, B.B., Arthur, M.A., 1994. Early Turonian paleogeographic/paleobathymetric map, Western Interior, U.S In: Caputo, M.V., Peterson, J.A., Franczyk, K.J. (Eds.), Mesozoic systems of the Rocky Mountain Region, USA. Rocky Mountain Section SEPM Special Publication, pp. 457–459.
Sageman, B.B., Meyers, S.R., Arthur, M.A., 2006. Orbital time scale and new C-isotope record for Cenomanian–Turonian boundary stratotype. Geology 34 (2), 125–128.
Shamrock, J.L., Watkins, D.K., 2009. Evolution of the Cretaceous calcareous nannofossil genus *Eiffellithus* and its biostratigraphic significance. Cretac. Res. 30, 1083–1102.
Sikora, P.J., Howe, R.W., Gale, A.S., Stein, J.A., 2004. Chronostratigraphy of proposed Turonian–Coniacian (Upper Cretaceous) stage boundary stratotypes: Salzgitter–Salder, Germany, and Wagon Mound, New Mexico, USA. In: Beaudoin, A.B., Head, M.J. (Eds.), The palynology and micropaleontology of boundaries. Geological Society, London, Special Publications, 230, pp. 207–242.
Smith, C.C., 1981. Calcareous nannoplankton and stratigraphy of Late Turonian, Coniacian, and early Santonian Age of the Eagle Ford and Austin Groups of Texas. Geol. Surv. Prof. Pap. 1075.
Styzen, M.J., 1997. Cascading counts of nannofossil abundance. J. Nannoplankton Res. 19 (1), 49.
Tantawy, A.A., 2008. Calcareous nannofossil biostratigraphy and paleoecology of the Cenomanian–Turonian transition in the Tarfaya Basin, southern Morocco. Cretac. Res. 29, 995–1007.
Tsikos, H., Jenkyns, H.C., Walsworth-Bell, B., Petrizzo, M.R., Forster, A., Kolonic, S., Erba, E., Premoli Silva, I., Baas, M., Wagner, T., 2004. Carbon-isotope stratigraphy recorded by the Cenomanian–Turonian Oceanic Anoxic Event: correlation and implications based on three key localities. J. Geol. Soc. Lond. 161, 711–719.
Varol, O., 1992. Taxonomic revision of the Polycyclolithaceae and its contribution to Cretaceous biostratigraphy. Newsl. Stratigr. 27 (3), 93–127.
Voigt, S., Erbacher, J., Mutterlose, J., Weiss, W., Westerhold, T., Wiese, F., Wilmsen, M., Wonik, T., 2008. The Cenomanian-Turonian of the Wunstorf section (North Germany): global stratigraphic reference section and new orbital time scale for Oceanic Anoxic Event 2. Newsletters on Stratigraphy 43 (1), 65–89.
Walaszczyk, I., Cobban, W.A., 2000. Inoceramid faunas and biostratigraphy of the Upper Turonian–Lower Coniacian of the Western Interior of the United States. Spec. Pap. Paleontol. 64, 1–118.
Walaszczyk, I., Lees, J.A., Peryt, D., Cobban, W.A., Wood, C.J., 2012. Testing the congruence of the macrofossil versus microfossil record in the Turonian–Coniacian boundary succession of the Wagon Mound–Springer composite section (NE New Mexico, USA). Acta Geol. Pol. 62 (4), 581–594.
Watkins, D.K., 1985. Biostratigraphy and paleoecology of calcareous nannofossils in the Greenhorn marine cycle. In: Pratt, L.M., Kauffman, E.G., Zelt, F.B. (Eds.), Fine-grained Deposits and Biofacies of the Cretaceous Western Interior Seaway: Evidence of Cyclic Sedimentary Processes: SEPM Field Trip Guidebook No. 4, pp. 151–156.
Watkins, D.K., 1986. Calcareous nannofossil paleoceanography of the Cretaceous Greenhorn Sea. GSA Bull. 97, 1239–1249.
Watkins, D.K., Bergen, J.A., 2003. Late Albian adaptive radiation in the calcareous nannofossil genus *Eiffellithus*. Micropaleontology 49, 231–252.
Watkins, D.K., Shafik, S., Shin, I.C., 1998. Calcareous nannofossils from the Cretaceous of the Deep Ivorian Basin. In: Lohmann, M.J., Moullade, M. (Eds.), Proceedings of the Ocean Drilling Program, Scientific Results, 159, pp. 319–333.
Wise, S., 1983. Mesozoic and Cenozoic calcareous nannofossils recovered by Deep Sea Drilling Project Leg 71 in the Falkland Plateau Region, Southwest Atlantic Ocean. In: Blakeslee, J.H., Lee, M. (Eds.), Initial Reports of the Deep Sea Drilling Project, 71, pp. 481–550.